

Oxamato-Bridged Trinuclear Ni^{II}Cu^{II}Ni^{II} Complexes: A New (Ni^{II}Cu^{II}Ni^{II})₂ Hexanuclear Complex and Supramolecular Structures. Characterization and Magnetic Properties

Javier Tercero,[†] Carmen Diaz,^{*†} Joan Ribas,[†] Miguel Maestro,[‡] José Mahía,[‡] and Helen Stoeckli-Evans[§]

Departament de Química Inorgànica, Universitat de Barcelona, Martí i Franquès 1-11, 08028-Barcelona, Spain, Institut de Chimie, Université de Neuchâtel, Avenue de Bellevaux 51, CH 2000 Neuchâtel, Switzerland, and Servicios Xerais de Apoio á Investigación, Facultade de Ciencias, Universidade da Coruña, Campus da Zapateira s/n. 15071-A Coruña, Spain

Received December 13, 2002

Eight oxamato-bridged heterotrinnuclear Ni^{II}Cu^{II}Ni^{II} complexes of formula $\{[\text{Ni}(\text{H}_2\text{O})(\text{dpt})]_2(\mu\text{-Cu}(\text{H}_2\text{O})(\text{opba}))\}(\text{ClO}_4)_2$ (**1**), $\{[\text{Ni}(\text{H}_2\text{O})(\text{dien})]_2(\mu\text{-Cu}(\text{pba}))\}(\text{ClO}_4)_2 \cdot 6\text{H}_2\text{O}$ (**2**), $\{[\text{Ni}(\text{H}_2\text{O})(\text{Medpt})]_2(\mu\text{-Cu}(\text{OHpba}))\}(\text{ClO}_4)_2 \cdot 4\text{H}_2\text{O}$ (**3**), $\{[\text{Ni}(\text{H}_2\text{O})(\text{dien})]_2(\mu\text{-Cu}(\text{Me}_2\text{pba}))\}(\text{ClO}_4)_2 \cdot 2.5\text{H}_2\text{O}$ (**4**), $\{[\text{Ni}(\text{H}_2\text{O})(\text{dpt})]_2(\mu\text{-Cu}(\text{Me}_2\text{pba}))\}(\text{ClO}_4)_2 \cdot 2\text{H}_2\text{O}$ (**5**), $\{[\text{Ni}(\text{H}_2\text{O})(\text{dien})]_2(\mu\text{-Cu}(\text{OHpba}))\}(\text{ClO}_4)_2 \cdot 4\text{H}_2\text{O}$ (**6**), $\{[\text{Ni}_2(\text{dpt})_2(\mu\text{-Cu}(\text{H}_2\text{O})(\text{pba}))]_2(\mu\text{-N}_3)_2\}\text{Na}_2(\text{ClO}_4)_4 \cdot 6\text{H}_2\text{O}$ (**7**), and $\{[\text{Cu}(\text{H}_2\text{O})_2(\text{dpt})\text{Ni}_2(\text{H}_2\text{O})(\text{dpt})_2]_2(\mu\text{-H}_2\text{Me}_2\text{pba}(2-))\}(\text{ClO}_4)_4 \cdot 3\text{H}_2\text{O}$ (**8**) in which opba = *o*-phenylenbis(oxamato), pba = 1,3-propylenebis(oxamato), OHpba = 2-hydroxy-1,3-propylenebis(oxamato), Me₂pba = 2,2-dimethyl-1,3-propylenebis(oxamato), dpt = 3,3'-diaminodipropylamine, dien = 2,2'-diaminodipropylamine, and Medpt = 3,3'-diamino-*N*-methyl dipropylamine were synthesized and characterized. The crystal structures of **1**, **7**, and **8** were solved. For complex **1**, the trinuclear entities are linked by hydrogen bonds forming a one-dimensional system, and for complex **8**, the presence of van der Waals interactions gives a one-dimensional system, too. For complex **7**, the trinuclear entities are self-assembled by azido ligands, given a hexanuclear system; each of these hexanuclear entities are self-assembled through two $[\text{Na}(\text{O})_3(\text{H}_2\text{O})_3]$ octahedral-sharing one-edge entities, given a one-dimensional system. The magnetic behavior of complexes **2–7** was investigated by variable-temperature magnetic susceptibility measurements. Complexes **2–6** exhibit the minimum characteristic of this kind of polymetallic species with an irregular spin state structure. The *J* value through the oxamato bridge varied between -88 cm^{-1} (for **6**) and -111.2 cm^{-1} (for **5**). For complex **7**, the values obtained were $J_1 = -101.7\text{ cm}^{-1}$ (through the oxamato ligand) and $J_2 = -3.2\text{ cm}^{-1}$ (through the azido ligand).

Introduction

Molecular magnetism has developed rapidly in the past two decades.^{1,2} Particular emphasis has been placed on the heterobimetallic complexes.^{3,4} A state of high-spin multiplicity in a polymetallic entity could be stabilized without

imposing ferromagnetic interactions between the nearest magnetic centers. To achieve this, two high local spins are aligned in the same direction due to antiferromagnetic interactions with a small spin located between them. The small central spin polarizes the two high terminal spins in a ferromagnetic-like fashion. The spin state structure of such complexes is said to be irregular in the sense that the spin associated with the low-lying states does not vary in a monotone fashion versus energy. Rather, when going down in energy, the spin first decreases and then increases. The χ_{MT} versus *T* plot reveals such behavior. The *N,N'*-substituted bis(oxamato)copper(II) complexes have an important function in the preparation of this kind of system.³ The use of these anionic mononuclear complexes and related ones in

* Author to whom correspondence should be addressed. E-mail: carme.diaz@qi.ub.es.

[†] Universitat de Barcelona.

[‡] Universidade da Coruña.

[§] Université de Neuchâtel.

(1) *Molecular Magnetism: From Molecular Assemblies to the Devices*; Coronado, E., Delhaès, P., Gatteschi, D., Müller, J. S., Eds.; Kluwer: Dordrecht, The Netherlands, 1996.

(2) Kahn, O. *Molecular Magnetism*, VCH: New York, 1993.

(3) Kahn, O. *Adv. Inorg. Chem.* **1995**, *43*, 179.

(4) Kahn, O. *Struct. Bonding (Berlin)*, **1987**, *68*, 89.

the “complex as a ligand” approach provided the preparation of several oxamato-bridged compounds: heterotrinnuclear complexes Mn^{II}Cu^{II}Mn^{II},^{5–7} Ni^{II}Cu^{II}Ni^{II},^{8–12} Co^{II}Cu^{II}Co^{II},¹³ and Fe^{III}Ni^{II}Fe^{III},^{14a} hexanuclear complex (Ni^{II}Cu^{II}Ni^{II})₂,^{14b} ferrimagnetic chains Mn^{II}Cu^{II},^{15,16} Ni^{II}Cu^{II},^{15,17} Fe^{II}Cu^{II},¹⁷ and Co^{II}Cu^{II},¹⁷ and more complex structures with radical species, Mn^{II}Cu^{II}^{18,19} and Co^{II}Cu^{II}.¹⁹ Despite the number of oxamato-bridged heterotrinnuclear systems reported, however, to our knowledge, only three Ni^{II}Cu^{II}Ni^{II} complexes have been characterized by X-ray crystallography: {[Ni(bapa)(H₂O)]₂-Cu(pba)}(ClO₄)₂ [bapa = bis(3-aminopropyl)amine and pba = 1,3-propylenebis(oxamato)] reported by some of us,⁸ {[Ni(bispictn)]₂Cu(pba)}(ClO₄)₂·2.5H₂O and {[Ni(cth)]₂Cu(pba)}(ClO₄)₂ [bispictn = *N,N'*-bis(2-pyridylmethyl)-1,3-propanediamine, cth = *rac*-5,7,7,12,14,14-hexamethyl-1,4,8,11-tetraazacyclotetradecane] recently reported by Gao et al.⁹ Only one heterohexanuclear (Ni^{II}Cu^{II}Ni^{II})₂ has been reported, but without crystal structure determination.^{14b}

One part of our research focused on whether the construction of coordination supramolecular arrays based on covalent interactions or hydrogen bonding for the rational design of functional materials could be controlled. The pathways used to obtain these species are based on the self-assembly method, using complexes as ligands. With homotrinnuclear Cu^{II}Cu^{II}Cu^{II} derived from substituted oxamato(2-) ligands, we described several supramolecular structures: hexanuclear systems,^{20a,b} one-dimensional systems,^{20b,c} and pseudo-two-dimensional systems.^{21,22} Parallel to the synthesis and

characterization of these homotrinnuclear complexes, we have worked for several years with heterotrinnuclear Ni^{II}Cu^{II}Ni^{II} systems, though only one compound has been fully characterized.⁸ We suggest several reasons for the difficulty of full characterization of this kind of complex: (a) The first precipitate that we found in each synthesis was a neutral dinuclear of general formula [Ni(amine)Cu(oxamato)]. One of these complexes, [Ni(cth)Cu(opba)]·CH₃OH, previously described by us,⁸ has been recently characterized through X-ray crystallography by Gao et al.⁹ This feature implies a change in the initial stoichiometry. (b) In most syntheses, the elemental analysis was not consistent with a well-characterized product, and the repetition of the synthetic method gave different analytical results. This feature implies the simultaneous synthesis of different kinds of products. (c) The crystallinity of these heterotrinnuclear Ni^{II}Cu^{II}Ni^{II} complexes is very low. The formation of oils during synthesis is frequent. In some cases, even, their power X-ray diffractograms show amorphous behavior. This feature indicated the difficulty of obtaining good crystals for X-ray studies. In this paper, we report the synthesis and magnetic properties of six trinuclear oxamato-bridged Ni^{II}Cu^{II}Ni^{II} species. Their formula are {[Ni(H₂O)(dpt)]₂(μ-Cu(H₂O)(opba))}(ClO₄)₂ (**1**), {[Ni(H₂O)(dien)]₂(μ-Cu(pba))}(ClO₄)₂·6H₂O (**2**), {[Ni(H₂O)(Medpt)]₂(μ-Cu(OHpba))}(ClO₄)₂·4H₂O (**3**), {[Ni(H₂O)(dien)]₂(μ-Cu(Me₂pba))}(ClO₄)₂·2.5H₂O (**4**), {[Ni(H₂O)(dpt)]₂(μ-Cu(Me₂pba))}(ClO₄)₂·2H₂O (**5**), and {[Ni(H₂O)(dien)]₂(μ-Cu(OHpba))}(ClO₄)₂·4H₂O (**6**), in which opba = *o*-phenylenebis(oxamato), pba = 1,3-propylenebis(oxamato), OHpba = 2-hydroxy-1,3-propylenebis(oxamato), Me₂pba = 2,2-dimethyl-1,3-propylenebis(oxamato), dpt = 3,3'-diaminodipropylamine, dien = 2,2'-diaminodiethylamine, and Medpt = 3,3'-diamino-*N*-methyldipropylamine. A hexanuclear complex, obtained from a self-assembly process between the trinuclear {[Ni₂(dpt)₂(H₂O)₂(μ-Cupba)](ClO₄)₂ system and azido group acting as bridging ligand, is also reported. The hexanuclear complexes are self-assembled through two [Na(O)₃(H₂O)₃] octahedral-sharing one-edge entities, given a one-dimensional system. Its formula is {[Ni₂(dpt)₂(μ-Cu(H₂O)(pba))]₂(μ-N₃)₂]Na₂(ClO₄)₄·6H₂O (**7**). We also characterized a secondary product of the formula {[Cu(H₂O)₂(dpt)Ni₂(H₂O)(dpt)₂(μ-H₂Me₂pba(2-))}(ClO₄)₄·3H₂O (**8**), in one of the attempts to synthesize complex **5**. The crystal structures of **1**, **7**, and **8** were determined. The magnetic properties of complexes **2–7** were studied.

Experimental Section

Materials and Synthesis. All the starting chemicals were A. R. grade and used as received. The mononuclear precursors, Na₂[Cu(pba)]·6H₂O,²³ Na₂[Cu(opba)]·3H₂O,²⁴ Na₂[Cu(OHpba)]·3H₂O,²⁵ and Na₂[Cu(Me₂pba)]·3H₂O,²⁶ were prepared as described in the literature.

- (5) Pei, Y.; Journaux, Y.; Kahn, O. *Inorg. Chem.* **1988**, *27*, 399.
- (6) Pei, Y.; Journaux, Y.; Dei, A.; Kahn, O.; Gatteschi, D. *J. Chem. Soc., Chem. Commun.* **1986**, 1300–1301.
- (7) Fettuouhi, M.; Ouahab, L.; Boukhari, A.; Cador, O.; Mathonière, C.; Kahn, O. *Inorg. Chem.* **1966**, *35*, 4932.
- (8) Ribas, J.; Diaz, C.; Costa, R.; Journaux, Y.; Mathonière, C.; Kahn, O.; Gleizes, A. *Inorg. Chem.* **1990**, *29*, 2042.
- (9) Gao, E. Q.; Tang, J. K.; Liao, D. Z.; Jiang, Z. H.; Yan, S. P.; Wang, G. L. *Inorg. Chem.* **2001**, *40*, 3134–3140.
- (10) Vicente, R.; Escuer, A.; Ribas, J. *Polyhedron* **1992**, *11*, 857.
- (11) Miao, M. M.; Cheng, P.; Liao, D. Z.; Jiang, Z. H.; Wang, G. L. *Transition Met. Chem.* **1996**, *41*, 995.
- (12) Miao, M. M.; Cheng, P.; Liao, D. Z.; Jiang, Z. H.; Wang, G. L. *Transition Met. Chem.* **1997**, *22*, 19.
- (13) Miao, M. M.; Cheng, P.; Liao, D. Z.; Jiang, Z. H.; Wang, G. L. *Transition Met. Chem.* **1997**, *22*, 330.
- (14) (a) Chaudhuri, P.; Winter, M.; Della Vedova, B. P. C.; Fleischauer, P.; Haase, W.; Flörke, U.; Haupt, H. *Inorg. Chem.* **1991**, *30*, 4777. (b) Aukauloo, A.; Ottenwaelder, X.; Ruiz, R.; Journaux, Y.; Pei, Y.; Rivière, E.; Muñoz, M. C. *Eur. J. Inorg. Chem.* **2000**, 951.
- (15) Pei, Y.; Verdager, M.; Kahn, O.; Sletten, J.; Renard, J. P. *Inorg. Chem.* **1987**, *26*, 138.
- (16) Baron, V.; Gillon, B.; Cousson, A.; Mathonière, C.; Kahn, O.; Grand, A.; Öhrström, L.; Delley, B.; Bonnet, M.; Boucherle, J. X. *J. Am. Chem. Soc.* **1997**, *119*, 3500.
- (17) Koningsbruggen, P.; Kahn, O.; Nakati, K.; Pei, Y.; Renard, J. P.; Drillon, M.; Legoll, P. *Inorg. Chem.* **1990**, *29*, 3325.
- (18) Stumpf, H. O.; Ouahab, L.; Bergerat, P.; Kahn, O. *J. Am. Chem. Soc.* **1994**, *116*, 3866.
- (19) Vaz, M. G. F.; Pinheiro, L. M. M.; Stumpf, H. O.; Alcântara, A. F. C.; Golhen, S.; Ouahab, L.; Cador, O.; Mathonière, C.; Kahn, O. *Chem. Eur. J.* **1999**, *5*, 1486.
- (20) (a) Tercero, J.; Diaz, C.; El Fallah, M. S.; Ribas, J.; Maestro, M. A.; Mahía, J. *Inorg. Chem.* **2001**, *40*, 3077. (b) Tercero, J.; Diaz, C.; Ribas, J.; Mahía, J.; Maestro, M. *Inorg. Chem.* **2002**, *41*, 5373. (c) Tercero, J.; Diaz, C.; Ribas, J.; Mahía, J.; Maestro, M.; Solans, X. *J. Chem. Soc., Dalton Trans.* **2002**, 2040.
- (21) Ribas, J.; Diaz, C.; Solans, X.; Font-Bardía, M. *Inorg. Chim. Acta* **1995**, *231*, 229.
- (22) Ribas, J.; Diaz, C.; Solans, X.; Font-Bardía, M. *J. Chem. Soc., Dalton Trans.* **1997**, 35.

- (23) Nonoyama, K.; Ojima, H.; Nonoyama, M. *Inorg. Chim. Acta* **1976**, *20*, 127.
- (24) Stumpf, H. O.; Pei, Y.; Kahn, O.; Sletten, J.; Renard, J. P. *J. Am. Chem. Soc.* **1993**, *115*, 6738.
- (25) Kahn, O.; Pei, Y.; Verdager, M.; Renard, J.; Sletten, J. *J. Am. Chem. Soc.* **1988**, *110*, 782.
- (26) Costa, R.; Garcia, A.; Sanchez, R.; Ribas, J.; Solans, X.; Rodriguez, V. *Polyhedron* **1993**, *12*, 2704.

Caution! Perchlorate and azido complexes of metal ions are potentially explosive. Only a small amount of material should be prepared, and this should be handled with caution.

$\{[\text{Ni}(\text{H}_2\text{O})(\text{dpt})]_2(\mu\text{-Cu}(\text{H}_2\text{O})(\text{opba}))\}(\text{ClO}_4)_2$ (**1**). An aqueous solution (20 mL) of dpt (4 mmol) was added to an aqueous solution (20 mL) of $\text{Ni}(\text{ClO}_4)_2 \cdot 6\text{H}_2\text{O}$ (4 mmol). To this mixture was added an aqueous solution (40 mL) of $\text{Na}_2[\text{Cu}(\text{opba})] \cdot 3\text{H}_2\text{O}$ (2 mmol). The mixture was stirred at room temperature for 1 h. After filtration to remove any impurities, the solution was left undisturbed, and few, but well-formed, blue crystals of **1** were obtained after several days. Compound **1** is the very minor product, and it is accompanied by a large amount of other compounds, all the separation attempts being unsuccessful.

$\{[\text{Ni}(\text{H}_2\text{O})(\text{dien})]_2(\mu\text{-Cu}(\text{pba}))\}(\text{ClO}_4)_2 \cdot 2.5\text{H}_2\text{O}$ (**2**). The complex was prepared in the same way as **1**, using dien and $\text{Na}_2[\text{Cu}(\text{pba})] \cdot 6\text{H}_2\text{O}$ instead of dpt and $\text{Na}_2[\text{Cu}(\text{opba})] \cdot 3\text{H}_2\text{O}$, respectively, but all our efforts to grow single crystals failed. Anal. Calcd for $\text{C}_{15}\text{H}_{45}\text{Cl}_2\text{Cu}_1\text{N}_8\text{Ni}_2\text{O}_{18.5}$: C, 20.35; H, 5.12; N, 12.65. Found: C, 20.5; H, 5.0; N 12.7.

$\{[\text{Ni}(\text{H}_2\text{O})(\text{Medpt})]_2(\mu\text{-Cu}(\text{OHpba}))\}(\text{ClO}_4)_2 \cdot 3\text{H}_2\text{O}$ (**3**). The complex was prepared in the same way as **1**, using Medpt and $\text{Na}_2[\text{Cu}(\text{OHpba})] \cdot 3\text{H}_2\text{O}$ instead of dpt and $\text{Na}_2[\text{Cu}(\text{opba})] \cdot 3\text{H}_2\text{O}$, but all our efforts to grow single crystals failed. Anal. Calcd for $\text{C}_{21}\text{H}_{52}\text{Cl}_2\text{Cu}_1\text{N}_8\text{Ni}_2\text{O}_{17}$: C, 26.81; H, 5.57; N, 11.9. Found: C, 26.6; H, 5.4; N, 11.7.

$\{[\text{Ni}(\text{H}_2\text{O})(\text{dien})]_2(\mu\text{-Cu}(\text{Me}_2\text{pba}))\}(\text{ClO}_4)_2 \cdot 2.5\text{H}_2\text{O}$ (**4**). The complex was prepared in the same way as **1**, using dien and $\text{Na}_2[\text{Cu}(\text{Me}_2\text{pba})] \cdot 3\text{H}_2\text{O}$ instead of dpt and $\text{Na}_2[\text{Cu}(\text{opba})] \cdot 3\text{H}_2\text{O}$, respectively, but all our efforts to grow single crystals failed. Anal. Calcd for $\text{C}_{17}\text{H}_{49}\text{Cl}_2\text{Cu}_1\text{N}_8\text{Ni}_2\text{O}_{18.5}$: C, 22.35; H, 5.41; N, 12.27. Found: C, 22.4; H, 5.2; N, 12.1.

$\{[\text{Ni}(\text{H}_2\text{O})(\text{dpt})]_2(\mu\text{-Cu}(\text{Me}_2\text{pba}))\}(\text{ClO}_4)_2 \cdot 2\text{H}_2\text{O}$ (**5**). The complex was prepared in the same way as **1**, using $\text{Na}_2[\text{Cu}(\text{Me}_2\text{pba})] \cdot 3\text{H}_2\text{O}$ instead of $\text{Na}_2[\text{Cu}(\text{opba})] \cdot 3\text{H}_2\text{O}$, but all our efforts to grow single crystals failed. Anal. Calcd for $\text{C}_{21}\text{H}_{56}\text{Cl}_2\text{Cu}_1\text{N}_8\text{Ni}_2\text{O}_{18}$: C, 26.25; H, 5.88; N, 11.66. Found: C, 26.4; H, 5.6; N 11.7.

$\{[\text{Ni}(\text{H}_2\text{O})(\text{dien})]_2(\mu\text{-Cu}(\text{OHpba}))\}(\text{ClO}_4)_2 \cdot 4\text{H}_2\text{O}$ (**6**). The complex was prepared in the same way as **3**, using dien instead of Medpt, but all our effort to grow single crystals failed. Anal. Calcd for $\text{C}_{15}\text{H}_{48}\text{Cl}_2\text{Cu}_1\text{N}_8\text{Ni}_2\text{O}_{21}$: C, 19.41; H, 5.21; N, 12.07. Found: C, 19.5; H, 5.1; N 11.9.

$\{[\text{Ni}_2(\text{dpt})_2(\mu\text{-H}_2\text{O})(\text{Cupba})]_2(\mu\text{-N}_3)_2\} \text{Na}_2(\text{ClO}_4)_4 \cdot 6\text{H}_2\text{O}$ (**7**). To an aqueous solution (50 mL) of $\{[\text{Ni}_2(\text{dpt})_2(\text{H}_2\text{O})_2(\mu\text{-Cupba})](\text{ClO}_4)_2\}$ previously reported by us⁸ (1.36 mmol) was added, an aqueous solution (20 mL) of NaN_3 (1.36 mmol) with constant stirring. The resulting solution was filtered to remove any impurity and left to evaporate slowly at room temperature. Dark-blue monocrystals suitable for X-ray determination were collected after 2 weeks. Anal. Calcd for $\text{C}_{38}\text{H}_{96}\text{Cl}_4\text{Cu}_2\text{N}_{22}\text{Na}_2\text{Ni}_4\text{O}_{36}$: C, 22.97; H, 4.87; N, 15.51. Found: C, 23.1; H, 4.9; N 15.6.

$\{[\text{Cu}(\text{H}_2\text{O})_2(\text{dpt})\text{Ni}_2(\text{H}_2\text{O})(\text{dpt})_2(\mu\text{-H}_2\text{Me}_2\text{pba}(2-))\}(\text{ClO}_4)_4 \cdot 3\text{H}_2\text{O}$ (**8**). The complex was obtained as secondary byproduct in one of the attempts to synthesize complex **5**. A few dark-blue monocrystals suitable for X-ray determination were collected. Repeated efforts controlling the pH value to synthesize this product, for magnetic measurements and elemental analysis, failed.

Crystal Structure Determination. Complexes 1 and 8. Suitable crystals of **1** (block, blue, dimensions $0.25 \times 0.15 \times 0.10 \text{ mm}^3$) and **8** (block, blue, dimensions $0.50 \times 0.25 \times 0.20 \text{ mm}^3$) were used for the determination of structure. X-ray data were collected using a Bruker SMART CCD area detector single-crystal diffractometer with graphite monochromatized Mo K α radiation ($\lambda = 0.71073 \text{ \AA}$) by the φ - ω scan method at 298 K for **1** and **8**. A total

of 1271 frames of intensity data were collected for **1** and **8**. The first 50 frames were re-collected at the end of data collection to be monitored for decay. The crystal used for the diffraction studies showed no decomposition during data collection. The integration process gave a total of 19175 reflections of which 7959 [$R(\text{int}) = 0.0839$] were independent for **1** and 31308 reflections, of which 10650 [$R(\text{int}) = 0.063$] were independent for **8**. Absorption corrections used the SADABS^{27a} program (maximum and minimum transmission coefficients, 1.000 and 0.738 for **1**, and 0.7752 and 0.5535 for **8**). The structures were solved using the Bruker SHELXTL-PC^{27b} software by direct methods and refined by full-matrix least-squares methods on F^2 . Hydrogen atoms were included in calculated positions and refined in the riding mode, except those of water molecules that were not included for **1** and except those of amines and water molecules that were located on residual density maps, but then fixed their positions and refined in the riding mode for **8**. For **1**, convergence was reached at a final $R1 = 0.0649$ [for $I > 2\sigma(I)$], $wR2 = 0.1594$ [for all data], 469 parameters, and for **8**, convergence was reached at a final $R1 = 0.0668$ [for $I > 2\sigma(I)$], $wR2 = 0.2004$ [for all data], 766 parameters, 311 restraints, with allowance for thermal anisotropy for all non-hydrogen atoms. The weighting scheme employed was $w = [\sigma^2(F_o^2 + (0.0677P)^2)]$ and $P = (|F_o|^2 + 2|F_c|^2)/3$, and the goodness of fit on F^2 was 1.107 for all observed reflections for **1**; $w = [\sigma^2(F_o^2 + (0.112P)^2)]$ and $P = (|F_o|^2 + 2|F_c|^2)/3$ and the goodness of fit on F^2 was 0.991 for all observed reflections for **8**.

Complex 7. A suitable crystal of **7** (block, blue, dimensions $0.40 \times 0.15 \times 0.10 \text{ mm}^3$) was used for the determination of structure. The intensity data were collected at 223 K on a Stoe image plate diffraction system^{28a} using Mo K α graphite monochromated radiation: image plate distance 70 mm, ϕ oscillation scans $0-200^\circ$, step $\Delta\phi = 1.0^\circ$, 2θ range $3.27-52.1^\circ$, $d_{\text{max}}-d_{\text{min}} = 12.45-0.81 \text{ \AA}$. The structure was solved by direct methods using the program SHELXS-97.^{27b} The refinement and all further calculations were carried out using SHELXL-97.^{28b} The water H-atoms could not be located. The remainder of the H-atoms were included in calculated positions and treated as riding atoms using SHELXL default parameters. The non-H atoms were refined anisotropically, using weighted full-matrix least-squares on F^2 . The crystal was a twin with almost 35% of the reflections overlapping. With the TWIN integration routine in the IPDS software, only the reflections for the major component of the twin were used for refinement.

Crystal data for complexes **1**, **7**, and **8**, and details on the data collection and refinement, are summarized in Table 1.

Physical Measurements. Magnetic measurements were carried out on polycrystalline samples with a SQUID magnetometer. The magnetic field was 1000 G. The diamagnetic corrections were estimated from Pascal tables.

Results and Discussion

Description of the Structure of 1. Complex **1** consists of heterotrinnuclear $\{[\text{Ni}(\text{H}_2\text{O})(\text{dpt})]_2(\mu\text{-Cu}(\text{H}_2\text{O})(\text{opba}))\}^{2+}$ cations and perchlorate anions. A perspective of the trinnuclear cation is depicted in Figure 1, and selected bond lengths and angles are listed in Table 2.

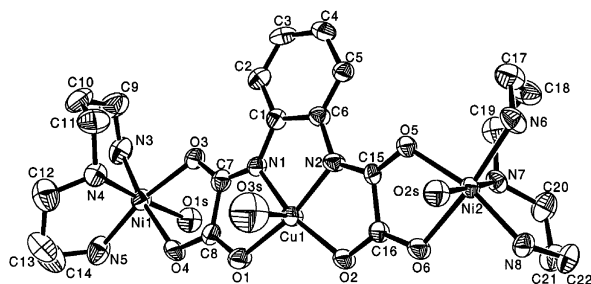
(27) (a) Sheldrick, G. M. *SADABS-Program for Empirical Absorption Correction of Area Detector Data*; University of Göttingen: Göttingen, Germany, 1996. (b) Sheldrick, G. M. *SHELXTL-97*; University of Göttingen: Göttingen, Germany, 1997.

(28) (a) *IPDS Software*; Stoe & Cie GmbH: Darmstadt, Germany, 2000. (b) Sheldrick, G. M. *SHELXL-97*; University of Göttingen: Göttingen, Germany, 1999.

Table 1. Crystallographic Data for Complexes **1**, **7**, and **8**

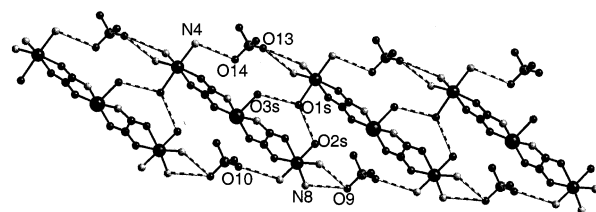
	1	7	8
formula	C ₂₂ H ₄₀ Cl ₂ ⁻ CuN ₈ Ni ₂ O ₁₇	C ₃₈ H ₈₈ Cl ₄ Cu ₂ ⁻ N ₂₂ Na ₂ Ni ₄ O ₃₆	C ₂₇ H ₅₆ Cl ₄ Cu ⁻ N ₁₁ Ni ₂ O ₂₈
fw	940.48	1979.00	1305.59
space group	<i>Pna</i> 2 ₁	<i>P</i> $\bar{1}$	<i>P2</i> ₁ / <i>n</i>
Z	4	1	4
<i>a</i> , Å	9.964(1)	8.657(1)	12.593 (1)
<i>b</i> , Å	12.834(1)	13.441(1)	33.359(1)
<i>c</i> , Å	28.122(1)	16.953(1)	13.147(1)
α , deg	90	85.05(1)	90
β , deg	90	82.396(9)	92.669(1)
γ , deg	90	86.480(9)	90
<i>V</i> , Å ³	3596.10(7)	1945.6(3)	5517.0(4)
ρ_{calcd} , g/cm ³	1.737	1.689	1.572
μ_{calcd} , mm ⁻¹	1.853	1.731	1.342
λ (Mo K α), Å	0.71073	0.71073	0.71073
<i>T</i> , K	298(2)	223(2)	298(2)
final <i>R</i> ^a indices	R1 = 0.0649	R1 = 0.0610	R1 = 0.0668
[<i>I</i> > 2 σ (<i>I</i>)]	wR2 = 0.1312	wR2 = 0.1598	wR2 = 0.1713
final <i>R</i> indices	R1 = 0.1188	R1 = 0.1072	R1 = 0.1327
[for all data]	wR2 = 0.1594	wR2 = 0.1732	wR2 = 0.2004

$$^a R1 = \sum ||F_o| - |F_c|| / \sum |F_o|. wR2 = \{ \sum (w(F_o^2 - F_c^2)^2) / \sum (w(F_o^2)^2) \}^{1/2}.$$

**Figure 1.** ORTEP view of the cationic part of $\{[\text{Ni}((\text{H}_2\text{O})(\text{dpt}))_2(\mu\text{-Cu}(\text{H}_2\text{O})(\text{opba}))](\text{ClO}_4)_2 \cdot \text{H}_2\text{O}$ (**1**) with the atom-labeling scheme. Ellipsoids are shown at the 50% probability level.**Table 2.** Selected Bond Lengths [Å] and Angles [deg] for **1**

Cu(1)–N(1)	1.908(6)	Ni(1)–O(4)	2.142(6)
Cu(1)–N(2)	1.914(6)	Ni(1)–O(1S)	2.205(6)
Cu(1)–O(1)	1.984(6)	Ni(2)–O(5)	2.052(5)
Cu(1)–O(2)	1.995(5)	Ni(2)–N(8)	2.071(6)
Cu(1)–O(3S)	2.421(11)	Ni(2)–N(6)	2.091(7)
Ni(1)–N(5)	2.062(8)	Ni(2)–N(7)	2.106(7)
Ni(1)–N(3)	2.064(8)	Ni(2)–O(6)	2.143(5)
Ni(1)–O(3)	2.092(6)	Ni(2)–O(2S)	2.259(6)
Ni(1)–N(4)	2.094(7)		
N(1)–Cu(1)–N(2)	83.4(2)	N(3)–Ni(1)–O(1S)	86.0(3)
N(1)–Cu(1)–O(1)	84.0(3)	O(3)–Ni(1)–O(1S)	87.9(2)
N(2)–Cu(1)–O(2)	84.3(2)	O(4)–Ni(1)–O(1S)	87.3(3)
N(1)–Cu(1)–O(3S)	99.0(3)	O(5)–Ni(2)–N(6)	94.0(3)
N(2)–Cu(1)–O(3S)	89.4(3)	N(8)–Ni(2)–N(6)	98.9(3)
O(1)–Cu(1)–O(3S)	90.2(3)	O(5)–Ni(2)–N(7)	87.8(2)
O(2)–Cu(1)–O(3S)	87.1(3)	N(8)–Ni(2)–N(7)	97.0(3)
N(5)–Ni(1)–N(3)	96.8(3)	N(6)–Ni(2)–N(7)	90.2(3)
N(3)–Ni(1)–O(3)	94.4(3)	O(5)–Ni(2)–O(6)	79.8(2)
N(5)–Ni(1)–N(4)	96.7(3)	N(8)–Ni(2)–O(6)	87.1(2)
N(3)–Ni(1)–N(4)	93.0(3)	N(7)–Ni(2)–O(6)	92.6(2)
O(3)–Ni(1)–N(4)	88.2(3)	O(5)–Ni(2)–O(2S)	90.4(2)
N(5)–Ni(1)–O(4)	88.5(3)	N(8)–Ni(2)–O(2S)	84.8(2)
O(3)–Ni(1)–O(4)	79.7(2)	N(6)–Ni(2)–O(2S)	90.1(3)
N(4)–Ni(1)–O(4)	93.3(3)	N(7)–Ni(2)–O(2S)	178.2(2)
N(5)–Ni(1)–O(1S)	87.4(3)	O(6)–Ni(2)–O(2S)	87.0(2)

In the trinuclear cation, the oxamato group bridges the Cu^{II} atom and the Ni^{II} atoms. The central Cu(1) ion has 4 + 1 coordination. Two oxygen atoms and two nitrogen atoms from the oxamato ligand form their basal plane; the fifth ligand is a water molecule. Their coordination polyhedron

**Figure 2.** Projection in the *xz* plane of the best view of the one-dimensional $\{[\text{Ni}((\text{H}_2\text{O})(\text{dpt}))_2(\mu\text{-Cu}(\text{H}_2\text{O})(\text{opba}))](\text{ClO}_4)_2$ (**1**) system.

is a square pyramid with a *t* factor value of 0.02;²⁹ the distance of the Cu^{II} atom to the basal plane is 0.037 Å. Both terminal Ni^{II} atoms are in a distorted octahedral environment. Their basal planes are formed by two nitrogen atoms (N(3), N(5) for Ni(1) and N(6), N(8) for Ni(2)) from the dpt ligand and two oxygen atoms (O(3), O(4) for Ni(1) and O(5), O(6) for Ni(2)) from the oxamato ligand. The two remaining positions are provided by the other nitrogen atom (N(4) for Ni(1) and N(7) for Ni(2)) from the dpt ligand and a water molecule, O(1S) for Ni(1) and O(2S) for Ni(2). The dpt ligand adopts the *fac* conformation for the two Ni^{II} ions. The Ni(1)–Cu(1)–Ni(2) angle is 165.96°, and the angle formed by the two oxamato-like planes (which contain the Ni^{II} and Cu^{II} atoms) is 167.8°. Intramolecular separations between metal ions are Cu(1)⋯Ni(1) = 5.347 Å and Cu(1)⋯Ni(2) = 5.327 Å. In the crystal (Figure 2), the trinuclear entities are self-assembled through hydrogen bonds from the oxygen atom O(1S) from the apical water molecule of Ni(1) of one entity, and the O(2S) and O(3S) from the apical water molecules from the Cu(1) and Ni(2), respectively, of the neighboring entity, thus leading to a chain along the *a* axis. On the chain, the distances between O(1S)–O(2S) and O(1S)–O(3S) are 2.95 and 2.97 Å, respectively. The perchlorate anions are linked by hydrogen bonding through two of their oxygen atoms, O(9) and O(10) of Cl(1) and O(13) and O(14) of Cl(2), and nitrogen atoms from the dpt blocking ligand. As shown in Figure 2, the perchlorate anions act as a passage of the chain. The structural data of these hydrogen bonds are shown in Table 1 (in the Supporting Information). The shortest intermolecular separation is Cu(1)⋯Ni(1) = 5.333 Å.

Description of the Structure of 7. Complex **7** consists of hexanuclear $\{[\text{Ni}_2(\text{dpt})_2(\mu\text{-Cu}(\text{H}_2\text{O})(\text{pba}))_2(\mu\text{-N}_3)_2\}^{2+}$ cations, complexed sodium metal cations, perchlorate anions, and solvent water molecules, both coordinated and noncoordinated. A perspective of the hexanuclear cation is depicted in Figure 3, and selected bond lengths and angles are listed in Table 3. The hexanuclear cation shows two trinuclear $\{[\text{Ni}_2(\text{dpt})_2(\mu\text{-Cupba})]^{2+}$ entities linked by two azido bridging ligands (Ni–N₃–Ni). The coordination polyhedron of Cu(1) is a square pyramid with a *t* factor value of 0.05.²⁹ The two oxygens and the two nitrogens of the pba ligand are placed in the basal position; the fifth ligand is a water molecule. The distance of the Cu^{II} atom from the basal plane is 0.17 Å. The Cu–N and Cu–O distances are close to 2.0 Å. The Ni^{II} atoms are in a distorted octahedral environment.

(29) Addison, A. W.; Rao, T. N.; Reedijk, J.; Rijn, J. V.; Verschoor, G. C. *J. Chem. Soc., Dalton Trans.* **1984**, 1349.

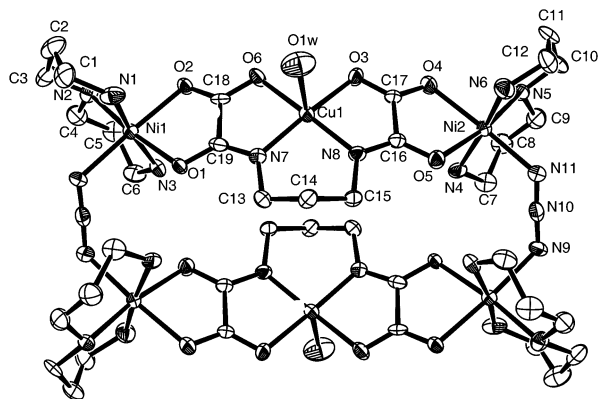


Figure 3. ORTEP view of the cationic part of $\{[\text{Ni}_2(\text{dpt})_2(\mu\text{-Cu}(\text{H}_2\text{O})\text{-}(\text{pba}))_2(\mu\text{-N}_3)_2]\text{Na}_2(\text{ClO}_4)_4 \cdot 6\text{H}_2\text{O}$ (**7**) with the atom labeling scheme. Ellipsoids are drawn at the 50% probability level.

Table 3. Selected Bond Lengths [Å] and Angles [deg] for **7**^a

Cu(1)–O(3)	1.992(6)	Ni(2)–N(11)	2.105(8)
Cu(1)–N(8)	1.918(7)	Ni(2)–O(4)	2.109(7)
Cu(1)–O(6)	1.977(6)	Ni(2)–N(4)	2.083(8)
Cu(1)–N(7)	1.926(8)	Ni(2)–N(6)	2.074(9)
Cu(1)–O(1W)	2.472(9)	Na(1)–O(3W)	2.483(12)
Ni(1)–O(2)	2.112(5)	Na(1)–O(6)	2.351(7)
Ni(1)–N(2)	2.096(7)	Na(1)–O(2W)#2	2.367(9)
Ni(1)–N(9)#	2.113(7)	Na(1)–O(3)	2.616(8)
Ni(1)–O(1)	2.098(6)	Na(1)–O(2W)	2.406(10)
Ni(1)–N(1)	2.069(9)	Na(1)–O(21)	2.483(12)
Ni(1)–N(3)	2.076(10)	N(9)–N(10)	1.167(11)
Ni(2)–O(5)	2.092(6)	N(10)–N(11)	1.187(11)
Ni(2)–N(5)	2.114(7)		
O(3)–Cu(1)–O(6)	93.4(2)	O(2)–Ni(1)–N(3)	88.7(3)
O(3)–Cu(1)–N(8)	83.9(3)	N(1)–Ni(1)–N(9)#1	90.9(3)
O(6)–Cu(1)–N(7)	84.2(3)	N(2)–Ni(1)–N(9)#1	91.9(3)
N(7)–Cu(1)–N(8)	96.7(3)	O(4)–Ni(2)–N(4)	89.6(3)
O(3)–Cu(1)–O(1W)	96.2(3)	O(4)–Ni(2)–N(6)	88.4(3)
O(6)–Cu(1)–O(1W)	87.6(3)	O(5)–Ni(2)–N(6)	85.5(3)
N(7)–Cu(1)–O(1W)	95.3(3)	N(4)–Ni(2)–N(5)	92.7(3)
N(8)–Cu(1)–O(1W)	101.1(3)	N(5)–Ni(2)–N(6)	96.3(3)
O(1)–Ni(1)–N(1)	86.2(3)	N(6)–Ni(2)–N(11)	87.1(3)
O(1)–Ni(1)–N(9)#1	94.3(3)	O(4)–Ni(2)–O(5)	80.3(2)
O(2)–Ni(1)–N(2)	93.0(3)	O(4)–Ni(2)–N(5)	90.3(3)
N(1)–Ni(1)–N(2)	94.0(3)	O(5)–Ni(2)–N(4)	85.3(3)
N(2)–Ni(1)–N(3)	95.5(3)	O(5)–Ni(2)–N(11)	92.9(3)
N(3)–Ni(1)–N(9)#1	92.6(3)	N(4)–Ni(2)–N(11)	93.9(3)
O(1)–Ni(1)–O(2)	80.8(2)	N(5)–Ni(2)–N(11)	96.6(3)
O(1)–Ni(1)–N(3)	84.0(3)	N(9)–N(10)–N(11)	177.0(9)
O(2)–Ni(1)–N(1)	87.0(3)		

^a Symmetry transformations used to generate equivalent atoms (#): 1, $-x + 2, -y, -z + 1$.

The four positions coplanar to the oxamato bridge are occupied by two oxygen atoms of this ligand, one nitrogen of the tridentate amine and one nitrogen of the azido bridge. The two remaining positions are occupied by the two other nitrogen atoms of the tridentate amine. The dpt ligand adopts the *mer* conformation for the two Ni^{II} ions. The angles formed by the azido-bridged ligands and the two Ni atoms of each trinuclear unit, which determine the magnetic properties at low temperatures (see later), are Ni(1)–N(9)–N(10) = 121.7° and N(10)–N(11)–Ni(2) = 122.9°. The angle in the azido bridge is N(9)–N(10)–N(11) = 177.0°. The Cu[⋯]Ni distances through the oxamato bridge are 5.323 Å, the Ni(1)[⋯]Ni(2) distances through the azido bridge are 5.028 Å, and the Cu(1)[⋯]Cu(1) distance in the hexanuclear entity is 6.078 Å. The hexanuclear complexes are self-

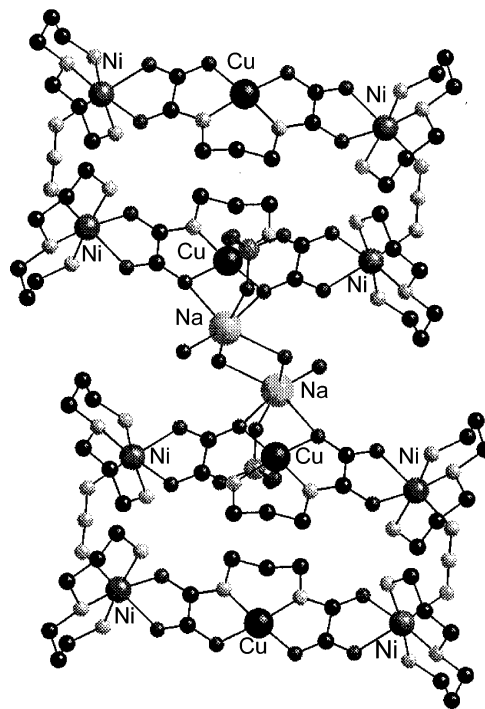


Figure 4. Projection in the xz plane of the best view of the one-dimensional $\{[\text{Ni}_2(\text{dpt})_2(\mu\text{-}(\text{H}_2\text{O})(\text{Cupba}))_2(\mu\text{-N}_3)_2]\text{Na}_2(\text{ClO}_4)_4 \cdot 6\text{H}_2\text{O}$ (**7**).

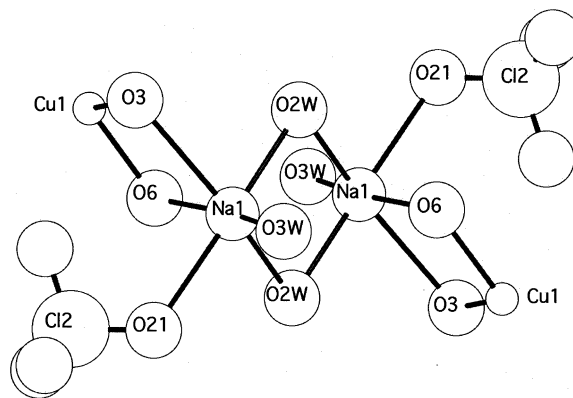


Figure 5. Diagram of the coordination of the sodium cations of $\{[\text{Ni}_2(\text{dpt})_2(\mu\text{-}(\text{H}_2\text{O})(\text{Cupba}))_2(\mu\text{-N}_3)_2]\text{Na}_2(\text{ClO}_4)_4 \cdot 6\text{H}_2\text{O}$ (**7**).

assembled through two $[\text{Na}(\text{O})_3(\text{H}_2\text{O})_3]$ octahedral-sharing one-edge entities, given a one-dimensional system. The bonds involved in the self-assembly process of the hexanuclear entities are shown in Figure 4. In each hexanuclear entity, two oxygen atoms of the oxamato ligand, O(3) and O(6), participate in the coordination of the sodium cations. As shown in Figure 5, the sodium cations of the neighboring hexanuclear units are linked to two water molecules acting as bridging ligands through O(2W). The sodium atoms are hexacoordinated, and the two remaining positions are occupied by a water molecule acting as terminal ligand through O(3W) and one oxygen atom of a neighboring perchlorate anion, O(21). The Na[⋯]Na distance is 3.442 Å, and the Cu[⋯]Cu distance through the two $[\text{Na}(\text{O})_3(\text{H}_2\text{O})_3]$ octahedral-sharing one-edge entities is 7.886 Å.

It should be emphasized that this kind of structure, first, the hexanuclear entity, and, second, the supramolecular one-dimensional architecture through hydrated Na⁺ cations, has

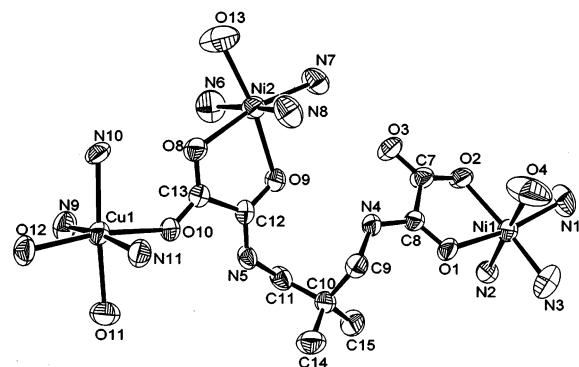


Figure 6. ORTEP view of the cationic part of $\{[\text{Cu}(\text{H}_2\text{O})_2(\text{dpt})\text{Ni}_2(\text{H}_2\text{O})_2(\text{dpt})_2](\mu\text{-H}_2\text{Me}_2\text{pba}(2-))\}(\text{ClO}_4)_4 \cdot 3\text{H}_2\text{O}$ (**8**) with the atom labeling scheme. Ellipsoids are drawn at the 50% probability level.

Table 4. Selected Bond Lengths [Å] and Angles [deg] for **8**

Ni(1)–N(1)	2.063(5)	Ni(2)–O(8)	2.119(4)
Ni(1)–N(2)	2.071(5)	Ni(2)–O(13)	2.129(6)
Ni(1)–N(3)	2.075(6)	Ni(2)–O(9)	2.131(4)
Ni(1)–O(1)	2.075(4)	Cu(1)–N(11)	2.057(5)
Ni(1)–O(2)	2.082(4)	Cu(1)–N(9)	2.069(5)
Ni(1)–O(4)	2.300(7)	Cu(1)–N(10)	2.099(5)
Ni(2)–N(6)	2.072(7)	Cu(1)–O(10)	2.111(4)
Ni(2)–N(8)	2.072(6)	Cu(1)–O(12)	2.114(4)
Ni(2)–N(7)	2.106(5)	Cu(1)–O(11)	2.170(5)
N(1)–Ni(1)–N(2)	96.9(2)	N(7)–Ni(2)–O(13)	99.7(2)
N(1)–Ni(1)–N(3)	96.7(3)	O(8)–Ni(2)–O(13)	91.9(2)
N(2)–Ni(1)–N(3)	97.0(2)	N(6)–Ni(2)–O(9)	89.8(3)
N(2)–Ni(1)–O(1)	91.6(2)	N(8)–Ni(2)–O(9)	91.4(2)
N(3)–Ni(1)–O(1)	88.3(2)	N(7)–Ni(2)–O(9)	90.0(2)
N(1)–Ni(1)–O(2)	94.2(2)	O(8)–Ni(2)–O(9)	78.47(15)
N(2)–Ni(1)–O(2)	93.4(2)	N(11)–Cu(1)–N(10)	94.7(2)
O(1)–Ni(1)–O(2)	79.17(16)	N(9)–Cu(1)–N(10)	94.5(2)
N(1)–Ni(1)–O(4)	90.1(2)	N(11)–Cu(1)–O(10)	87.7(2)
N(3)–Ni(1)–O(4)	76.3(3)	N(9)–Cu(1)–O(10)	88.27(18)
O(1)–Ni(1)–O(4)	82.2(2)	N(10)–Cu(1)–O(10)	92.91(17)
O(2)–Ni(1)–O(4)	91.9(2)	N(11)–Cu(1)–O(12)	90.9(2)
N(6)–Ni(2)–N(7)	94.6(2)	N(9)–Cu(1)–O(12)	91.72(19)
N(8)–Ni(2)–N(7)	94.9(2)	N(10)–Cu(1)–O(12)	96.22(19)
N(6)–Ni(2)–O(8)	87.2(2)	N(11)–Cu(1)–O(11)	85.7(2)
N(8)–Ni(2)–O(8)	83.6(2)	N(9)–Cu(1)–O(11)	84.9(2)
N(6)–Ni(2)–O(13)	87.9(3)	O(10)–Cu(1)–O(11)	82.72(17)
N(8)–Ni(2)–O(13)	89.4(3)	O(12)–Cu(1)–O(11)	88.15(18)

never been reported before. Journaux et al.³⁰ reported the synthesis of an oxamate-bridged Na^ICu^{II} three-dimensional coordination polymer, in which oxygen atoms of the oxamate participate in the coordination of the sodium metal cations.

Description of the Structure of 8. Complex **8** consists of trinuclear $\{[\text{Cu}(\text{H}_2\text{O})_2(\text{dpt})\text{Ni}_2(\text{H}_2\text{O})_2(\text{dpt})_2](\mu\text{-H}_2\text{Me}_2\text{pba}(2-))\}^{4+}$ cations, perchlorate anions, and solvent water molecules. A perspective of the trinuclear cation is depicted in Figure 6, and selected bond lengths and angles are listed in Table 4. In this complex, the starting fully deprotonated 2,2-dimethyl-1,3-propylenbis(oxamato)(4-) is protonated in the two strong basic amide-N species, N(5) and N(4), so that these nitrogen atoms remain uncoordinated. The oxamate ligand coordinates, as bridging ligand, with Ni(1) as κ^2 -O(1),O(2), with Ni(2) as κ^2 -O(9),O(8), and with Cu(1) as κ -O(10). The carbonyl O(3) atom remains uncoordinated. The two Ni atoms and the Cu atom are in a distorted

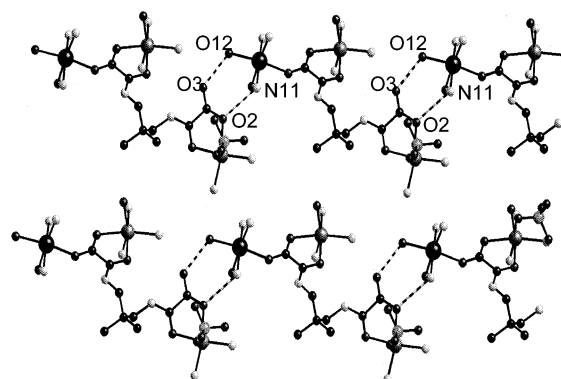


Figure 7. Projection in the yz plane of the best view of the one-dimensional $\{[\text{Cu}(\text{H}_2\text{O})_2(\text{dpt})\text{Ni}_2(\text{H}_2\text{O})_2(\text{dpt})_2](\mu\text{-H}_2\text{Me}_2\text{pba}(2-))\}(\text{ClO}_4)_4 \cdot 3\text{H}_2\text{O}$ (**8**).

octahedral environment. For Ni(1), Ni(2), and Cu(1), three of the four remaining positions are occupied by the three nitrogen atoms of the tridentate amine (dpt). An oxygen atom, O(4), of a neighboring perchlorate anion, completes the hexacoordination for Ni(1), an oxygen atom O(13) from a water molecule completes the hexacoordination of Ni(2), and two oxygen atoms O(11) and O(12) from water molecules complete the hexacoordination of Cu(1). The dpt ligand adopts the *mer* conformation for the Cu(1) and Ni(2) ions and the *fac* conformation for the Ni(1) ion. Intramolecular separations between metal ions are $\text{Cu}(1) \cdots \text{Ni}(2) = 5.662$ Å and $\text{Ni}(1) \cdots \text{Ni}(2) = 8.202$ Å. In the crystal (Figure 7), the trinuclear entities are self-assembled by van der Waals interactions between the carbonyl O(3) atom and the O(2) atom, from the oxamato ligand of one entity, and the oxygen atom O(12) from a water molecule and the nitrogen N(11) from the tridentate amine (dpt) from the Ni(1) of the neighboring entity, thus leading to a chain along the c axis. On the chain, the contact distances for O(3)–O(12) is 2.712 Å, and for O(2)–N(11) is 2.981 Å. The shortest metal–metal distance, Ni(1)–Cu(1), in the chain is 6.014 Å.

Magnetic Studies. Ni^{II}Cu^{II}Ni^{II} Species. The interaction through the oxamato ligand between Ni^{II} and Cu^{II} is antiferromagnetic. The spin state structure of Ni^{II}Cu^{II}Ni^{II} trinuclear species has already been discussed.⁸ It is irregular, and the energy of the low-lying states does not vary monotonically with spin. The ground state is a quartet, above which there are two doublets, another quartet, and one sextuplet. Such an irregular spin state structure is revealed by the χ_{MT} versus T plot, which exhibits a characteristic minimum. For the trinuclear complexes **2–6**, the χ_{MT} products decrease smoothly upon cooling, reach the expected minimum around 110–90 K with χ_{MT} at about $2.1 \text{ cm}^3 \text{ mol}^{-1}$ K, and increase smoothly upon cooling further. The expected χ_{MT} decrease at very low temperature, owing to the D parameter of the quartet ground state, was not observed, as was already reported for other trinuclear Ni^{II}Cu^{II}Ni^{II} complexes.⁸ On the contrary, the χ_{MT} values at low temperature are greater than those expected for an isolated Ni^{II}Cu^{II}Ni^{II} complex. The lack of structural data makes impossible the interpretation of this unexpected feature. Figure 8 shows the magnetic behavior of complex **6**. Magnetic behavior for complexes **2–5** is given in Figure S1 (Supporting Informa-

(30) Aukauloo, A.; Ottenwaelder, X.; Ruiz, R.; Journaux, Y.; Pei, Y.; Rivière, E.; Cervera, B.; Muñoz, M. C. *Eur. J. Inorg. Chem.* **1999**, 209.

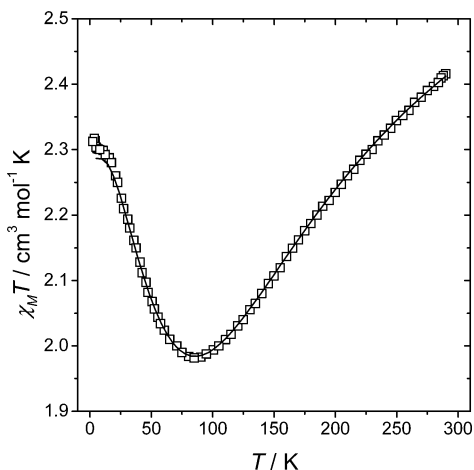


Figure 8. Experimental and calculated (—) variations of $\chi_M T$ versus T for $\{[\text{Ni}(\text{H}_2\text{O})(\text{dien})]_2(\mu\text{-Cu}(\text{OHpba}))\}(\text{ClO}_4)_2 \cdot 4\text{H}_2\text{O}$ (**6**).

Table 5. Magnetic Parameters for Complexes **2–6** and Some Previously Reported Species

complex	$J \text{ cm}^{-1}$	g_{Ni}	g_{Cu}	ref
$\{[\text{Ni}(\text{H}_2\text{O})(\text{dien})]_2(\mu\text{-Cu}(\text{pba}))\}(\text{ClO}_4)_2 \cdot 6\text{H}_2\text{O}$ (2)	-98.7	2.23	2.29	<i>a</i>
$\{[\text{Ni}(\text{H}_2\text{O})(\text{Medpt})]_2(\mu\text{-Cu}(\text{OHpba}))\}(\text{ClO}_4)_2 \cdot 4\text{H}_2\text{O}$ (3)	-102.2	2.12	2.24	<i>a</i>
$\{[\text{Ni}(\text{H}_2\text{O})(\text{dien})]_2(\mu\text{-Cu}(\text{Me}_2\text{pba}))\}(\text{ClO}_4)_2 \cdot 2.5\text{H}_2\text{O}$ (4)	-101.1	2.30	2.24	<i>a</i>
$\{[\text{Ni}(\text{H}_2\text{O})(\text{dpt})]_2(\mu\text{-Cu}(\text{Me}_2\text{pba}))\}(\text{ClO}_4)_2 \cdot 2\text{H}_2\text{O}$ (5)	-111.2	2.30	2.30	<i>a</i>
$\{[\text{Ni}(\text{H}_2\text{O})(\text{dien})]_2(\mu\text{-Cu}(\text{OHpba}))\}(\text{ClO}_4)_2 \cdot 4\text{H}_2\text{O}$ (6)	-88.8	2.3	2.3	<i>a</i>
$\{[\text{Ni}(\text{bapa})(\text{H}_2\text{O})]_2(\mu\text{-Cu}(\text{pba}))\}(\text{ClO}_4)_2^b$	-90.3	2.19	2.12	8
$\{[\text{Ni}(\text{bispictn})]_2(\mu\text{-Cu}(\text{pba}))\}(\text{ClO}_4)_2 \cdot 2.5\text{H}_2\text{O}^b$	-107.2	2.15	2.19	9
$\{[\text{Ni}(\text{cth})]_2(\mu\text{-Cu}(\text{pba}))\}(\text{ClO}_4)_2^b$	-109.2	2.13	2.15	9
$\{[\text{Ni}(\text{bispictn})]_2(\mu\text{-Cu}(\text{OHpba}))\}(\text{ClO}_4)_2 \cdot \text{H}_2\text{O}$	-102.0	2.13	2.15	9
$\{[\text{Ni}(\text{cth})]_2(\mu\text{-Cu}(\text{opba}))\}(\text{ClO}_4)_2 \cdot \text{H}_2\text{O}$	-104.2	2.13	2.18	9
$\{[\text{Ni}(\text{cth})]_2(\mu\text{-Cu}(\text{OHpba}))\}(\text{ClO}_4)_2$	-90.0	2.29	2.20	10
$\{[\text{Ni}(\text{Me}_3[12\text{N}_3])]_2(\mu\text{-Cu}(\text{Me}_2\text{pba}))\}(\text{ClO}_4)_2$	-110.0	2.30	2.32	10

^a This work. ^b The structure is reported.

tion). Thus, to fit experimental magnetic behavior, we used the Hamiltonian previously described by us,⁸ assuming the zero-field splitting parameter (D) of the ground state equal to zero. Fitting the experimental data to this expression and finishing it at ca. $2.2 \text{ cm}^3 \text{ mol}^{-1} \text{ K}$, which is the final plateau for an isolated trinuclear entity, leads to the parameters listed in Table 5. For comparative purposes, the parameters of some previously reported $\text{Ni}^{\text{II}}\text{-Cu}^{\text{II}}\text{-Ni}^{\text{II}}$ species are also listed. All attempts to fit the full experimental curve were unsuccessful, either assuming $D = 0$ or introducing the ZFS in the ground quartet state. The raised $\chi_M T$ values at low temperatures can be due to the possibility of weak ferromagnetic coupling between the trinuclear entities associated with structural parameters such as hydrogen bonds, as indicated in a previous work on similar trinuclear $\text{Ni}^{\text{II}}\text{Cu}^{\text{II}}\text{-Ni}^{\text{II}}$ complexes.^{14b}

Hexanuclear Complex. As shown in the crystallographic part, the hexanuclear complex is formed by two trinuclear entities linked by N_3^- bridging ligands (Figure 3). The two cases shown in Figure 9 are the two extremes used for analyzing experimental magnetic measurements and the treatment of data. If the magnetic interaction between these two entities is weakly ferromagnetic, at low temperatures

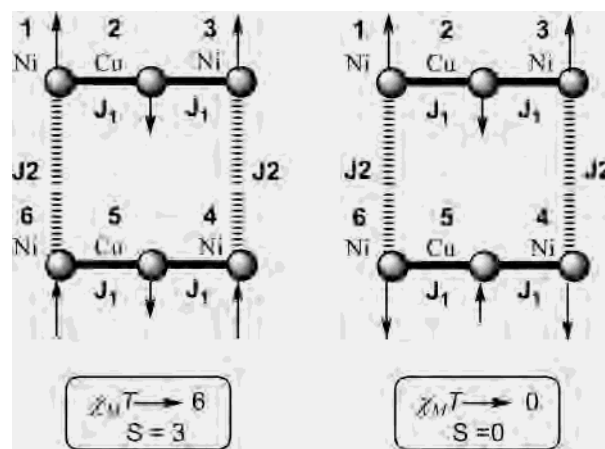


Figure 9. Scheme of the spin topology assuming intermolecular ferromagnetic (a) or antiferromagnetic (b) coupling in the hexanuclear system, $\{[\text{Ni}_2(\text{dpt})_2(\mu\text{-Cupba})]_2(\mu\text{-N}_3)_2\}^{2+}$

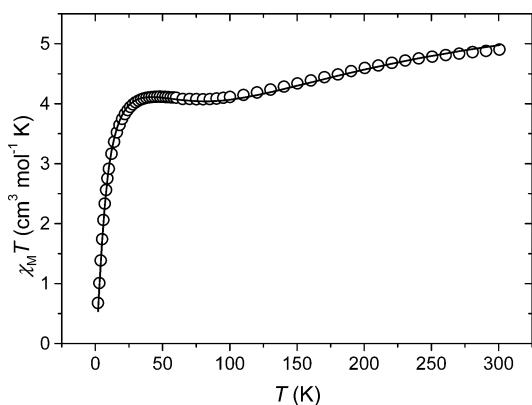


Figure 10. Experimental and calculated (—) variations of $\chi_M T$ versus T for $\{[\text{Ni}_2(\text{dpt})_2(\mu\text{-Cu}(\text{H}_2\text{O})(\text{pba}))]_2(\mu\text{-N}_3)_2\}\text{Na}_2(\text{ClO}_4)_4 \cdot 6\text{H}_2\text{O}$ (**7**).

the resulting S_T value tends to 3 and the $\chi_M T$ curve increases and tends to a value greater than 6 (with $g > 2.00$). However, if the coupling is weakly antiferromagnetic, the resulting S_T values tend to zero and the $\chi_M T$ curve decreases and tends to zero (Figure 9). The susceptibility measurements for complex **7** are shown in Figure 10. The fit of the experimental data was performed according to the following Hamiltonian:

$$H = -J_1(S_1S_2 + S_2S_3 + S_4S_5 + S_5S_6) - J_2(S_1S_6 + S_3S_4)$$

where J_1 corresponds to the coupling through the oxamato bridge, and J_2 to the coupling through the azido bridging between the trinuclear entities (Figure 9). The free parameters were J_1 , J_2 , and g (average). The fit made by the irreducible tensor operator formalism (ITO), using the CLUMAG program,³¹ gave the following results: $J_1 = -101.7 \text{ cm}^{-1}$, $J_2 = -3.2 \text{ cm}^{-1}$, $g = 2.27$, and $R = 1.7 \times 10^{-4}$. J_1 is the typical value for $\text{Ni}^{\text{II}}\text{-Cu}^{\text{II}}$ coupling in oxamato complexes. The low J_2 value (due to azido bridging ligands) agrees with those previously reported for this kind of Ni -azido complex. The two main parameters that affect the J value are the Ni-N-N angle and the $\text{Ni-N}_3\text{-Ni}$ torsion angle.³² The maximum antiferromagnetic J value is found for 108° and 110°

(31) Gatteschi, D.; Pardi, L. *Gazz. Chim. Ital.* **1993**, *123*, 231.

Ni–N–N angles, for *trans* and *cis* complexes, respectively.³² In complex **7**, the Ni–N–N angles are 121.7° and 122.9°, and the Ni–N₃–Ni torsion angle is 116.4° (with 180° considered the ideal planar geometry). This torsion angle, involving azido bridging ligands and Ni^{II} ions, is the greatest reported in the literature: the AF coupling must be small. In fact, it is -3.2 cm^{-1} , one of the lowest reported so far.³² Finally, to compare the theoretical magnetic behavior for the two extreme cases represented in Figure 9, a simulation of the $\chi_M T$ versus T , using the same formalism, was performed, with the J_1 value set as -102 cm^{-1} and the g value as 2.27 and the values of J_2 varying between -10 and 10 cm^{-1} (Figure S2, Supporting Information). When J_2 coupling is antiferromagnetic, $\chi_M T$ decreases when the temperature is lowered, tending to zero; when J_2 is ferromagnetic, $\chi_M T$ increases when the temperature is lowered, tending to a finite value greater than 6 because $g = 2.27$.

EPR Spectra. Complexes **2–6** show similar spectra, which vary with the temperature. The spectrum of complex **5** is shown in Figure 11a. At 4 K, it exhibits a resonance with a maximum at approximately 1000 G and a small signal at ca. 3200 G. Upon warming, the relative intensities of the signals decrease and become broader. The spectra of the remaining complexes are similar. These spectra are in good agreement with those expected for a Ni^{II}Cu^{II}Ni^{II} system: the spectrum at low temperature is associated with the Kramer doublet $\pm 1/2$ arising from the $S = 3/2$ ground state, which must present two signals approximately in the ratio $g_{\perp} \approx 2g_{\parallel}$.^{5,8–10} At room temperature, the spectrum is very broad due to overlap of the signals of all the excited populated states.

The EPR spectra for complex **7** (the hexanuclear complex) are more complicated (Figure 11b) due to the small exchange coupling ($J = -3.2\text{ cm}^{-1}$) between trinuclear entities, which give a new ground state $S = 0$ but with excited states $S = 1, 2,$ and 3 very close in energy. Thus, at least, the $S = 1$ excited state must be populated even at low temperature. These $S = 1$ states have an important zero-field splitting which is responsible for the pattern of the spectrum. Upon warming, the relative intensities of the signals decrease and become broader, due to the population of all excited states.

Conclusion

Working with the versatile N₃⁻ ligand, we were able to stabilize the first hexanuclear complex formed by two Ni^{II}-Cu^{II}Ni^{II} entities. The presence of the Na⁺ cations allowed the synthesis of a new unexpected supramolecular architecture, in which each [NaO₃(H₂O)₃] links together hexanuclear entities. All attempts to crystallize other similar complexes, with or without azido ligands, have failed for years. These

(32) Ribas, J.; Escuer, A.; Monfort, M.; Vicente, R.; Cortés, R.; Lezama, L.; Rojo, T. *Coord. Chem. Rev.* **1999**, *193–195*, 1027 and references therein.

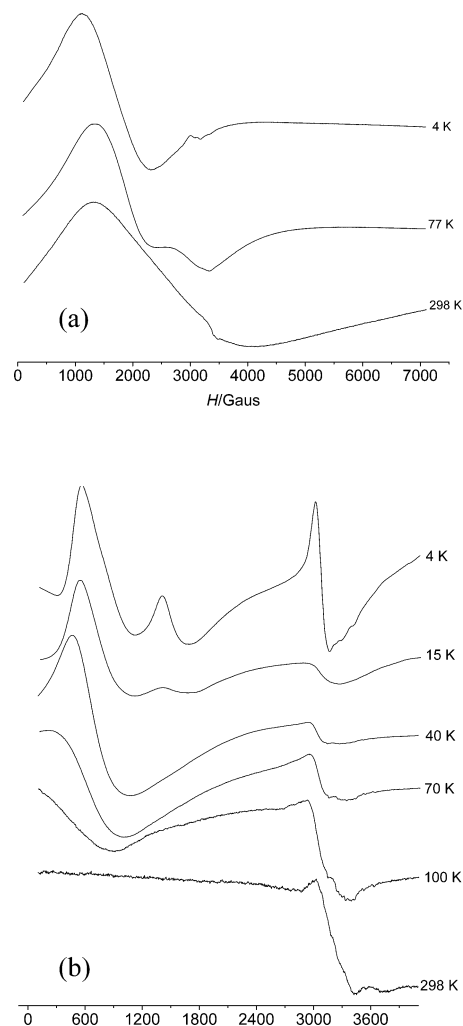


Figure 11. Polycrystalline EPR spectra for complexes **5** (a) and **7** (b). The intensities of the signals at 298 K are ca. 100 times less intense than at 4 K, for both complexes.

complexes show very poor crystallinity, and the analyses of most of them are not repeatable in different syntheses, due to the presence of unexpected compounds, one of them structurally determined. This is the major difference between this kind of complex and the similar Cu^{II}Cu^{II}Cu^{II} or Ni^{II}Cu^{II} derivatives, previously synthesized and reported by us and other authors (see Introduction), which show good crystallinity.

Acknowledgment. This study was supported by Grant BQU2000/0791 from the Dirección General de Investigación Científica y Técnica (Spanish Government).

Supporting Information Available: Additional table and figures and three X-ray crystallographic files, in CIF format. This material is available free of charge via the Internet at <http://pubs.asc.org>.

IC026264Z